Electrochimica Acta 54 (2009) 4893–4897

Contents lists available at ScienceDirect

Electrochimica Acta

journal homepage: www.elsevier.com/locate/electacta

Particle size effects of gold on the kinetics of the oxygen reduction at chemically prepared Au/C catalysts

Takeshi Inasaki, Shū Kobayashi*

Department of Chemistry, School of Science, The University of Tokyo, The HFRE Division, ERATO, Japan Science Technology Agency (JST), Hongo, Bunkyo-ku, Tokyo 113-0033, Japan

ARTICLE INFO

Article history:
Received 5 September 2008
Received in revised form 24 February 2009
Accepted 24 February 2009
Available online 9 March 2009

Keywords:
Gold on carbon
Particle size effects
Rotating ring-disk electrode
Oxygen reduction
Fuel cells

ABSTRACT

Gold nanoparticles with narrow and controlled size distributions have been synthesized chemically and deposited onto a carbon support. Using the resulting gold on carbon (Au/C) catalysts, Au particle size effects on the kinetics of the oxygen reduction reaction (ORR) were analyzed in acidic media (0.5 M H_2SO_4). From rotating ring-disk electrode (RRDE) voltammetric studies, it was found that, for bulk gold, the number of electrons, n, involved in the ORR was nearly constant at potentials above −0.2 V. On the contrary, for the catalysts with diameters less than 10–15 nm, the value of n increased as the potential became more negative, and the highest value of n was obtained when the size of Au particles was less than 3 nm. Those results showed that further reduction of H_2O_2 or direct 4-electron reduction of O_2 proceeded at relatively low overpotential on extremely small gold clusters.

1. Introduction

Bulk gold is known as one of the most inert metals in the periodic table according to activated chemisorption theory [1–4]. This feature is attributed to the lack of interaction between the orbitals of adsorbates like hydrogen or oxygen and the occupied d orbitals of bulk gold [5–6]. In 1989, pioneering work by Haruta et al. demonstrated that Au nanoclusters (<10 nm) dispersed on TiO_2 support displayed unexpectedly high activity toward CO oxidation [7] and propylene epoxidation [8]. Since then, exploration of gold nanoparticles in catalysis has attracted a wide range of interest from both the fundamental research and industrial development aspects [9–12]. Among the reactions catalyzed by gold, the oxygen reduction reaction (ORR) is an important process in fuel cell and other electrochemical devices. In general, the most widely used catalyst in fuel cells is platinum, as it supports the 4-electron reduction of O_2 at relatively low overpotentials [13]. However, because of its rareness on earth and consequent high cost, substitution from platinum to other catalysts has been widely studied [14–17], and gold based catalysts have been identified as candidate materials.

In general, gold is a much less active electrocatalyst for ORR in acidic media than in alkaline media [18–19], and in acidic media a 2-electron reduction of oxygen takes place on Au surface, while the peroxide intermediate is further reduced only at high overpotentials [20–21]. However, it was reported that the catalytic performance of the gold electrodes was found to depend markedly on the size of the gold particles, the nature of the support as well as the method of preparation. El-Deab and Ohsaka [22] showed that, in acidic solutions, the rate of both oxygen and H_2O_2 reduction are larger on Au nanoparticles (20–200 nm) electrodeposited on polycrystalline gold, than on bulk gold alone. Yagi et al. [23] reported that a significant positive shift of the oxygen reduction peak and increase in the current efficiency consumed for the 4-electron reduction were observed for smaller Au nanoparticles (>2 nm) deposited on boron-doped diamond electrodes. However, Guerin et al. [24] showed that small particles of gold with diameters below ∼3 nm were less active for oxygen reduction on carbon and titanium dioxide supports. Above this critical particle diameter, the catalytic activity became independent of particle size. Sarapuu et al. [25] prepared thin film gold electrodes by vacuum evaporation onto glassy carbon (GC), and showed that the number of electrons (n) involved in the ORR decreased as the Au film became thinner. Thus, at the present moment, it is not clear whether the O_2 reduction activity is improved by reducing the size of Au clusters and it is not clear whether the support materials affect the O_2 reduction activity.

The aim of the present work is to investigate the influence of cluster size of Au catalysts on the kinetics of oxygen reduction in acidic medium. For this purpose, we prepared Au/C catalysts with controlled Au size distributions using chemical reduction methods, and investigated their catalytic activities using rotating ring-disk electrode voltammetry.

* Corresponding author. Tel.: +81 3 5841 4790; fax: +81 3 5684 0634.
E-mail address: shu_kobayashi@chem.s.u-tokyo.ac.jp (S. Kobayashi).

0013-4686/$ – see front matter © 2009 Elsevier Ltd. All rights reserved.
doi:10.1016/j.electacta.2009.02.075

2. Experimental

2.1. Preparation of Au/C catalysts

Inductively coupled plasma analysis (ICP) was conducted with SHIMADZU ICPS-7510. Transmission electron microscope (TEM) images were obtained using JEOL JEM-1010 instrument operated at 80 kV. Carbon black (Ketjen Black EC, Ketjen Black International) with a specific surface area of 800 m^2/g was used.

2.1.1. Preparation from triphenylphosphine-protected gold sol

For the synthesis of the catalyst with the smallest Au, we used chloro(triphenylphosphine)gold as a gold precursor [26,27]. It is reported that triphenylphosphine acts as a good protecting group for gold sol, and it is used for syntheses of extremely small gold colloidal solutions (ca. 1–2 nm) [28].

To a suspension of carbon black (500 mg) in diglyme (50 mL) was added chloro(triphenylphosphine)gold (66.1 mg, 0.13 mmol), and the mixture was cooled to 0 °C. To this mixture was added $NaBH_4$ (50.5 mg, 1.3 mmol) solution in diglyme (7 mL) in one portion, then the mixture was stirred for 24 h at room temperature. The mixture was filtered, washed with water, methanol and dichloromethane then dried *in vacuo* to give the catalyst (510 mg). From ICP analyses, the contents of Au and P in the catalyst were determined; loading of gold metal: 0.22 mmol/g (4.3 wt.%), phosphorus moieties remained: 0.05 mmol/g. For complete removal of phosphorus moieties, the catalyst was treated with hydrogen peroxide. To a mixture of water:ethanol (5:2, 56 mL) was added the catalyst (400 mg), and the mixture was sonicated for 10 min, then cooled to 0 °C. 10% Aqueous H_2O_2 (60 mL) was added and the mixture was stirred for 2 h at 0 °C. The mixture was filtered, washed with ethanol and dichloromethane then dried *in vacuo* to give Au/C-a (396 mg); loading of gold metal: 0.24 mmol/g (4.7 wt.%), phosphorus moieties remained: n.d. (<0.04 mmol/g).

2.1.2. Preparation from citrate-protected gold sol

Sols generated in the presence of citrate were prepared by modifying the methods with two different types of reducing agents, citrate itself [29] and $NaBH_4$ [30], which controlled the Au particle sizes.

To an aqueous solution of hydrogen tetrachloroaurate tetrahydrate (44.1 mg, 0.107 mmol in 420 mL H_2O) cooled to 0 °C was added an aqueous trisodium citrate solution (42.2 mg, 0.14 mmol in 4 mL H_2O). After 5 min, a mixture of trisodium citrate (42.2 mg, 0.14 mmol) and $NaBH_4$ (3.2 mg, 0.085 mmol) in H_2O (0.85 mL) was added to the solution, then the mixture was stirred vigorously for 15 min. An ethanol dispersion of carbon black (400 mg in 40 mL EtOH) was added to this mixture, and the mixture was stirred for 20 min then filtered. The filtrate was washed with ethanol and water, dried *in vacuo* to give Au/C-b (408.3 mg); loading of gold metal: 0.24 mmol/g (4.7 wt.%).

To an aqueous solution of hydrogen tetrachloroaurate tetrahydrate (44.1 mg, 0.107 mmol in 440 mL H_2O) heated at 70 °C was added an aqueous trisodium citrate solution (210.2 mg, 0.71 mmol in 4 mL H_2O), and the mixture was stirred for 3 h at 70 °C. After cooling to room temperature, an ethanol dispersion of carbon black (400 mg in 40 mL EtOH) was added to this mixture, and the mixture was stirred for 20 min then filtered. The filtrate was washed with ethanol and water, dried *in vacuo* to give Au/C-c (415.2 mg); loading of gold metal: 0.24 mmol/g (4.7 wt.%).

2.2. Preparation of the Au/C-modified GC electrodes

GC disk (diameter = 4 mm)-Pt ring and Au disk (diameter = 4 mm)-Pt ring electrodes were used as a working electrode. They were polished to a mirror finish with 1.0 μm diamond and 0.05 μm alumina slurries. After polishing with alumina the electrodes were washed with Milli-Q water and methanol.

Au/C dispersion was prepared as follows. The Au/C catalyst (so that the Au content in the dispersion would become 0.15 g/L) and 5% Nafion solution (so that the Carbon:Nafion ratio would become 9:1 by weight) were added to a mixture of water:ethanol:2-propanol (2:1:1), and the mixture was sonicated for 30 min. A constant volume (3 μL in general) of the dispersion was transferred onto the GC disk electrode and underwent to drying at room temperature. Then, the electrode was heat-treated at 80 °C for 30 min in air.

2.3. Electrochemical measurements

Electrochemical measurements were carried out with a bipotentiostat (ALS/chi 704C). All the measurements were performed at room temperature (25 ± 1 °C). A platinum wire and a Ag/AgCl/KCl (sat.) were used as the counter electrode and the reference electrode, respectively. All electrode potentials were reported with respect to the Ag/AgCl/KCl (sat.). Prior to the ORR experiments, the working electrodes were electrochemically pretreated in 0.5 M H_2SO_4 solution by repeating the potential scan in the range of −0.2–1.5 V at 0.1 V/s several times (15 cycles in general) to clean the electrode surface. RDE and RRDE techniques were used to clarify the kinetics of oxygen reduction at Au nanoparticles and the potential dependency of H_2O_2 formation. The collection efficiency of the electrode was 0.31–0.34, which was measured using a solution of $Fe(CN)^{-3}$ [31]. The ring potential was kept at 1.0 V so that all H_2O_2 molecules that reached the ring were oxidized to O_2. The background current measured in Ar-saturated solution was subtracted from these data.

3. Results and discussion

3.1. Characterization of the catalysts

Representative TEM images of the catalysts and the corresponding histogram are shown in Fig. 1A–C and D, respectively. The Au particles of Au/C-a are nearly monodispersed with an average size of 1.7 ± 0.5 nm. In the cases of Au/C-b and Au/C-c, Au size distributions are a little larger (Au/C-b: 4.8 ± 2 nm, Au/C-c: 13.2 ± 2 nm) than that of Au/C-a, however, we could obtain the catalysts with three specific size distributions of gold particles.

The catalysts were characterized electrochemically by cyclic voltammetry (CV) as shown in Fig. 2. For the Au/C-modified GC electrodes, a large increase in the background current was observed in the presence of carbon black. The anodic peaks at 1.20 V corresponded to the formation of the Au surface oxides and the cathodic peak at 0.94 V to their reduction. For Au/C catalysts with smaller Au particle sizes, the cathodic peaks at 0.94 V were larger than those for the Au/C catalysts with larger Au particle sizes, due to higher surface area of the smaller particles.

3.2. Oxygen reduction

Because the ORR activity of carbon materials is typically very low in acidic media [32], the activity of the Au/C-modified catalysts is due to only the deposited Au particles. We first examined the effects of the catalyst loading on the ORR activity. Fig. 3 shows the RDE voltammograms for the ORR on Au/C-a-modified electrode with different loadings of the catalyst. The cathodic potential was limited to −0.2 V to avoid contamination with the H_2 evolution current or the reduction current for the carbon support. It was evident that the catalytic activity decreased with lower loading of the catalyst. From these results, we hereafter fixed the loading of the catalysts on GC electrode to a constant value (i.e. 0.45 μg of Au/electrode).

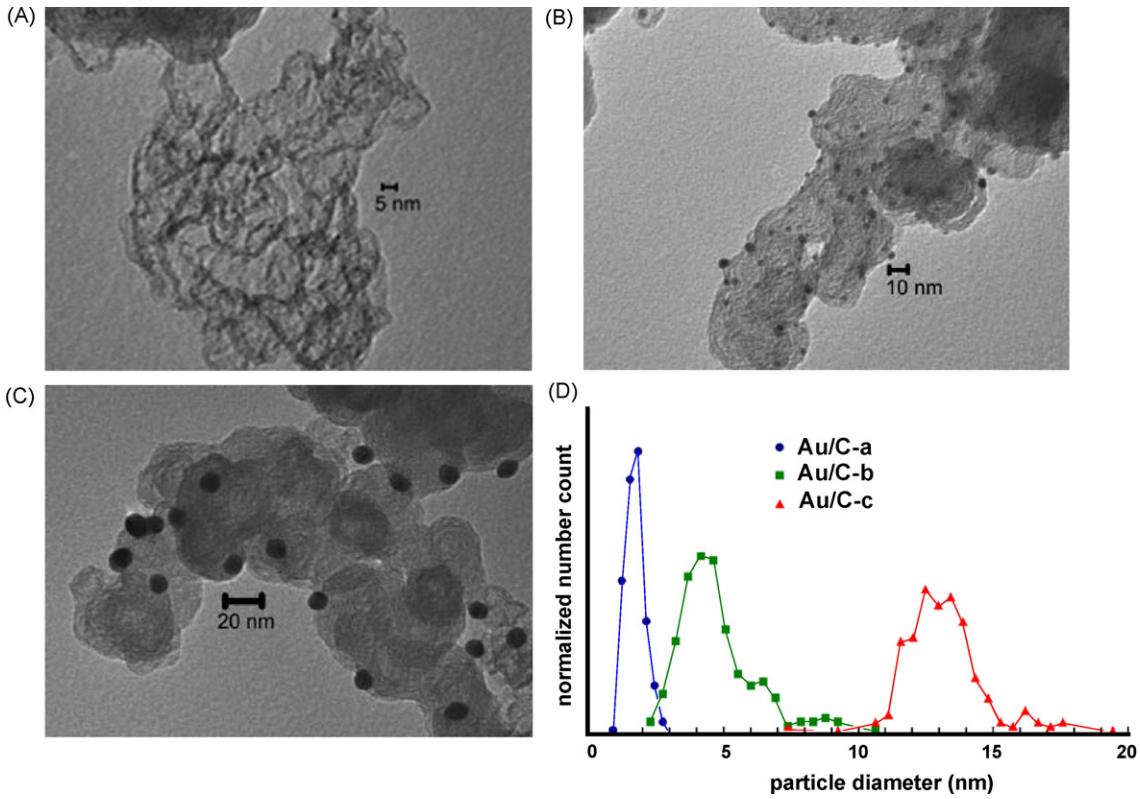

Fig. 1. TEM images of the Au/C catalysts used: (A) Au/C-a, (B) Au/C-b, (C) Au/C-c. (D) Particle size distributions of gold particles on the Au/C catalysts obtained from TEM measurements.

Fig. 4 shows the RDE voltammograms for the ORR on Au/C-a-modified electrode at different rotation rates, and these data were analyzed using the Koutechy–Levich (K–L) equation:

$$\frac{1}{i} = \frac{1}{i_k} + \frac{1}{i_d} = -\frac{1}{nFAkC^0} - \frac{1}{\{0.62nFAD_{O_2}{}^{2/3}\nu^{-1/6}C^0\omega^{1/2}\}} \quad (1)$$

where i is the measured current, i_k and i_d are the kinetic and diffusion-limited currents, respectively, k is the rate constant for the ORR, F is the Faraday constant (96484 C mol^{-1}), A is the effective projected area covered with catalysts, ω is the rotation rate, C^0 is the saturated concentration of oxygen in the bulk (1.13×10^{-6} mol cm^{-3}), D_{O_2} is the diffusion coefficient of oxygen (1.8×10^{-5} cm^2 s^{-1}) and ν is the kinematic viscosity of the solution (0.01 cm^2 s^{-1}) [33].

Fig. 5 shows the K–L plots obtained from the RDE data presented in Fig. 4. The slope of these lines decreased gradually as the potential shifted to a more negative value, indicating that the n value increased at more negative potentials. From the slope of the plots, we could not determine the n value precisely for the Au/C-modified GC disk electrodes due to a lack of exact A value [34]. Therefore we applied RRDE techniques to determine the exact n value.

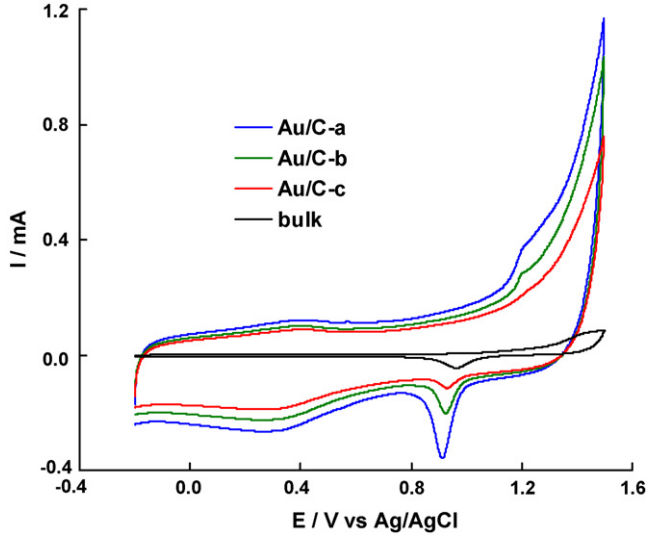

Fig. 2. Cyclic voltammograms for the Au/C-modified GC electrodes and bulk Au electrode in Ar-saturated 0.5 M H_2SO_4 at a scan rate of 100 mV s^{-1}. For the Au/C-modified electrodes, loading of Au metal on a GC electrode was fixed at 0.45 μg/electrode.

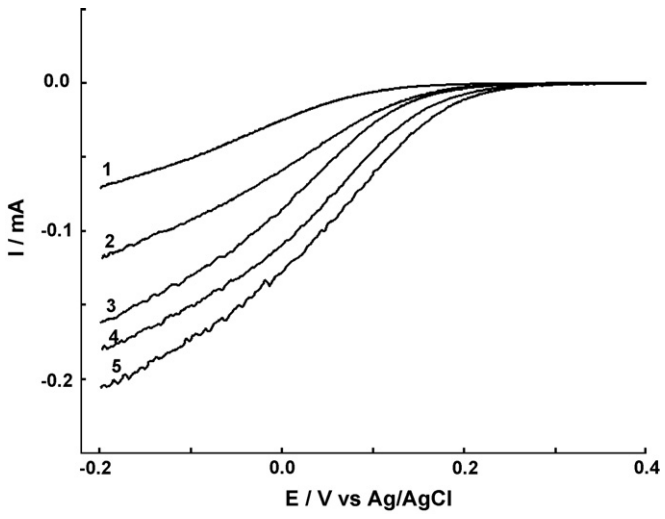

Fig. 3. RDE voltammograms for the oxygen reduction in O_2-saturated 0.5 M H_2SO_4 at the Au/C-a-modified GC electrode at a rotation rate of 500 rpm. Loading of Au metal on the electrode: (1) 0.15, (2) 0.30, (3) 0.45, (4) 0.68, (5) 0.90 μg. ν = 10 mV s^{-1}.

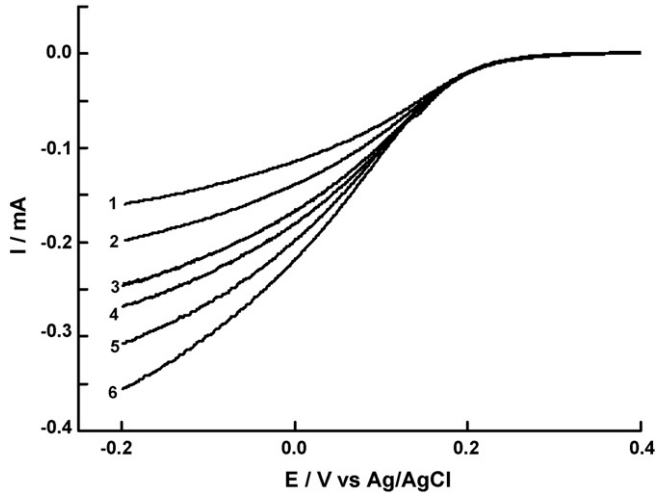

Fig. 4. RDE voltammograms for the oxygen reduction in O_2-saturated 0.5 M H_2SO_4 at the Au/C-a-modified GC electrode. Rotation rate: (1) 300, (2) 500, (3) 800, (4) 1000, (5) 1500, (6) 2000 rpm. $\nu = 10\,mV\,s^{-1}$.

To investigate the dependence of catalytic activity on Au cluster size, we obtained the specific activity (SA) at a given potential from Fig. 5. The value of SA was calculated using the following equation:

$$SA = \frac{i_k}{A_r} \quad (2)$$

where i_k is the kinetic current at a given potential and A_r is the real surface area of gold. The value of A_r was determined from Fig. 2, using a value of 400 μC cm^{-2} for the reduction of the surface oxide monolayer [35]. Thus obtained SA values at 0.10 V are 0.58 mA cm^{-2} (Au/C-a), 0.80 mA cm^{-2} (Au/C-b) and 1.05 mA cm^{-2} (Au/C-c), respectively. The values of SA decreased with decreasing Au cluster size. This observation is comparable with previous studies [24,25].

Since cathodic oxygen reduction is a multi-electron reaction associated with the formation of a large number of intermediates [36,37], it is difficult to consider all of them. We thus used a simplified model [38] shown in Fig. 6 to analyze experimental results in this study. Path 1 in Fig. 6 is the path where O_2 is reduced directly to

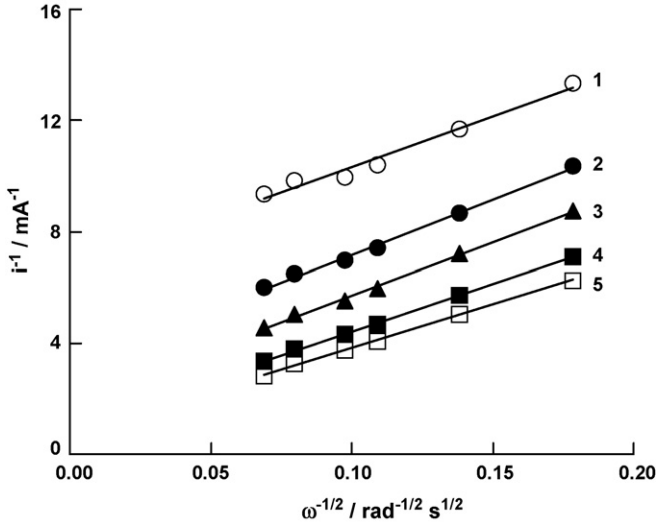

Fig. 5. K–L plots for the ORR on the Au/C-a-modified GC electrode in O_2-saturated 0.5 M H_2SO_4 at various potentials: (1) 0.10, (2) 0.05, (3) 0.00, (4) −0.10, (5) −0.20 V. Data derived from Fig. 4.

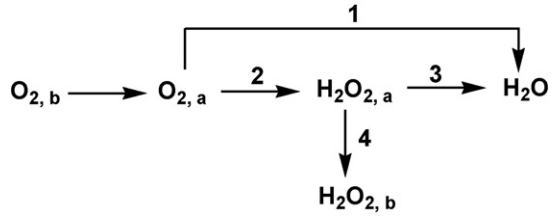

Fig. 6. Schematic illustration of the possible O_2 reduction pathways. The subscripts (a) and (b) mean adsorbed state and bulk solution species, respectively.

H_2O through 4-electron transfer. Path 2 is the sequential reaction path where O_2 is first reduced to H_2O_2 through 2-electron transfer followed by further 2-electron reduction to H_2O (Path 3), or by the release of formed H_2O_2 into bulk solution (Path 4).

Fig. 7 shows RRDE voltammograms for the ORR at bulk Au disk and different Au/C-modified GC disk electrodes at a rotation rate of 500 rpm. The current for the Pt ring electrode as a function of the disk electrode potential is shown at the upper side of Fig. 7 (curves marked a′–d′). As can be readily seen from this figure, the onset potential for the ORR shifts to more positive as the gold particle size is decreased, which shows that the overpotential for the ORR decreases with diminishing Au particle size. In addition, the ring currents for catalysts with smaller gold particles tend to decrease at a lower potential region, especially the ring current for Au/C-a-modified electrode shows a maximum at −0.05 V. These phenomena show that the partial change of the reaction mechanism, from 2- to 4-electron reduction, occurs at these electrodes. For further investigation, we calculated the number of electrons involved in the ORR from the data shown in Fig. 7, according to

$$n = 4 - \frac{2I_R}{NI_D} \quad (3)$$

where I_R and I_D were the ring and the disk currents respectively, and N was the collection efficiency, which was a parameter that only depended on the diameters of the ring and the disk and was equal to 0.31–0.34 for the present cases [18,39]. Fig. 8 shows the dependence of n on the potential for the ORR at bulk Au and different Au/C-modified GC electrodes. In the case of bulk gold, the value of n is nearly constant i.e. $n \sim 2$ at this potential range. However for the cases of the Au/C catalysts, the values of n tend to increase

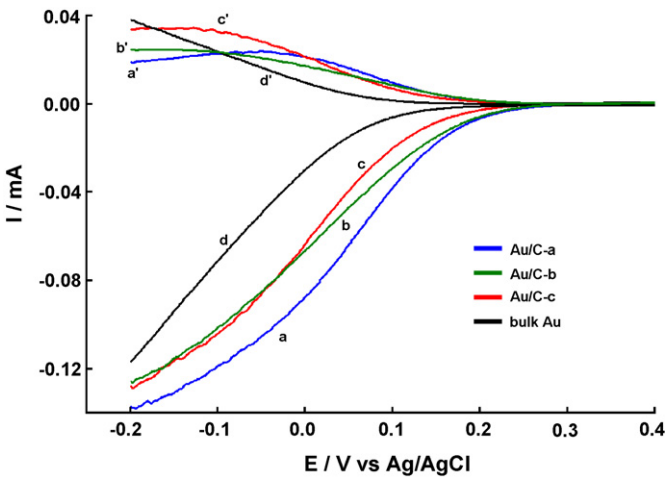

Fig. 7. RRDE voltammograms for the oxygen reduction in O_2-saturated 0.5 M H_2SO_4, at (a–c) the Au/C-modified GC electrodes and (d) bulk Au electrode at a rotation rate of 500 rpm. Curves a′–d′ represent the corresponding Pt-ring currents (polarized at 1.0 V). For the Au/C-modified electrodes, loading of Au metal on a GC electrode was fixed at 0.45 μg/electrode. $\nu = 10\,mV/s^{-1}$.

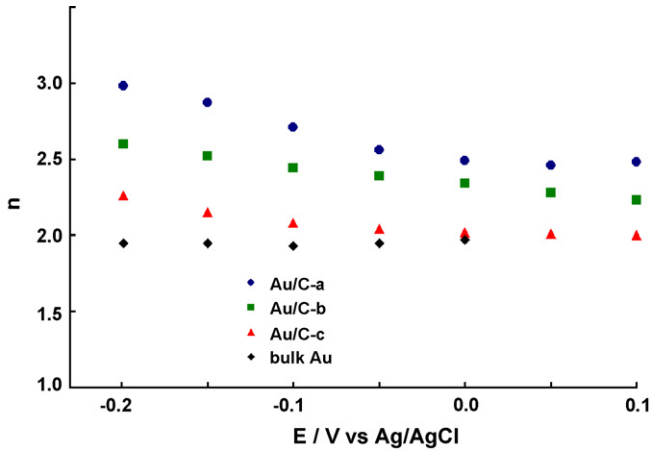

Fig. 8. Potential dependence of n for the Au/C-modified GC electrodes and bulk Au electrode in 0.5 M H_2SO_4.

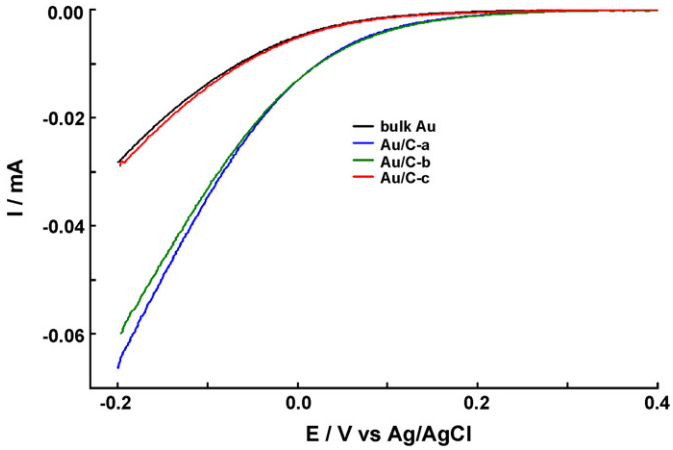

Fig. 9. RDE voltammograms for the H_2O_2 reduction in Ar-saturated 0.5 M H_2SO_4 solution with 5 mM H_2O_2 at (a–c) the Au/C-modified GC electrodes and (d) bulk Au electrode at a rotation rate of 500 rpm. For the Au/C-modified electrodes, loading of Au metal on a GC electrode was fixed at 0.45 μg/electrode. $\nu = 10$ mV s^{-1}.

as the potential becomes more negative, and reach to 2.3 (Au/C-c), 2.6 (Au/C-b) and 3.0 (Au/C-a) at −0.2 V. Previously higher n values compared with bulk Au were reported for nano-sized Au particles in acidic medium [22,23], and our results are in agreement with those observations. Furthermore, our data provides more precise information on the kinetics of the ORR on gold. For the case of Au particles with diameters less than ca. 10–15 nm, the value of n increases as the potential becomes more negative, and the highest value of n is obtained when the size of Au particles is less than 3 nm.

For further proof of higher reactivity on smaller Au particles, we examined the activity of H_2O_2 reduction at each electrode. Fig. 9 shows the RDE voltammograms in an Ar-saturated 0.5 M H_2SO_4 solution with 5 mM H_2O_2 at bulk Au and different Au/C-modified GC electrodes. In the case of Au/C-c, the reduction current was slightly increased compared with bulk gold. In the cases of Au/C-b and Au/C-a, though the onset potential of the ORR was nearly the same as that of bulk gold, the reduction currents were 2–2.6 times larger than that of bulk Au over the whole potential range. These results show that the 2-step 4-electron reduction of O_2 to H_2O proceeds more favorably on Au particles with diameters less than ca. 10 nm.

4. Conclusions

The particle size effects of gold catalysts on the oxygen reduction in acidic medium have been investigated. For this purpose, we chemically prepared gold nanoparticles with narrow and controlled size distributions and deposited onto a carbon support. The gold particles with the mean diameter 1.7 ± 0.5, 4.8 ± 2 and 13.2 ± 2 nm were synthesized. In the case of bulk gold, the value of n is nearly constant at potential above −0.2 V. On the other hand, the increase of n was observed for Au particles less than 10–15 nm as the potential shifted to more negative value, indicating that activity of the 2-step 4-electron reduction was high or the direct 4-electron reduction of O_2 to H_2O occurred. The maximum increase of n was observed when the particle size of Au was less than 3 nm.

Appendix A. Supplementary data

Supplementary data associated with this article can be found, in the online version, at doi:10.1016/j.electacta.2009.02.075.

References

[1] B. Hammer, J.K. Nørskov, Surf. Sci. 343 (1995) 211.
[2] B. Hammer, J.K. Nørskov, Nature 376 (1995) 238.
[3] J. Greeley, J.K. Nørskov, M. Mavrikakis, Annu. Rev. Phys. Chem. 53 (2002) 319.
[4] Z. Shi, J. Zhang, Z.-S. Liu, H. Wang, D.P. Wilkinson, Electrochim. Acta 51 (2006) 1905.
[5] G.C. Bond, Catal. Today 72 (2002) 5.
[6] R.J. Davis, Science 301 (2003) 926.
[7] M. Haruta, N. Yamada, T. Kobayashi, S. Iijima, J. Catal. 115 (1989) 301.
[8] T. Hayashi, K. Tanaka, M. Haruta, J. Catal. 178 (1998) 566.
[9] N. Dimitratos, J.A. Lopez-Sanchez, D. Morgan, A. Carley, L. Prati, G.J. Hutchings, Catal. Today 122 (2007) 317.
[10] S. Kanaoka, N. Yagi, Y. Fukuyama, S. Aoshima, H. Tsunoyama, T. Tsukuda, H. Sakurai, J. Am. Chem. Soc. 129 (2007) 12060.
[11] M.D. Hughes, Y.-J. Xu, P. Jenkins, P. McMorn, P. Landon, D.I. Enache, A.F. Carley, G.A. Attard, G.J. Hutchings, F. King, E.H. Stitt, P. Johnston, K. Griffin, C.J. Kiely, Nature 437 (2005) 1132.
[12] A.K. Sinha, S. Seelan, S. Tsubota, M. Haruta, Angew. Chem. Int. Ed. 43 (2004) 1546.
[13] U.A. Paulus, T.J. Schmidt, H.A. Gasteiger, R.J. Behm, J. Electroanal. Chem. 495 (2001) 134.
[14] B. Wang, J. Power Sources 152 (2005) 1.
[15] S.-Q. Liu, J.-Q. Xu, H.-R. Sun, D.-M. Li, Inorg. Chim. Acta 306 (2000) 87.
[16] R. Bashyam, P. Zelenay, Nature 443 (2006) 63.
[17] J. Ozaki, N. Kimura, T. Anahara, A. Oya, Carbon 45 (2007) 1847.
[18] M.S. El-Deab, T. Sotomura, T. Ohsaka, Electrochem. Commun. 7 (2005) 29.
[19] D. Jasin, Electrochim. Acta 52 (2007) 4581.
[20] M. Alvarez-Rizatti, K. Jüttner, J. Electroanal. Chem. 144 (1983) 351.
[21] S. Štrbac, R.R. Adžić, Electrochim. Acta 41 (1996) 2903.
[22] M.S. El-Deab, T. Ohsaka, Electrochim. Acta 47 (2002) 4255.
[23] I. Yagi, T. Ishida, K. Uosaki, Electrochem. Commun. 6 (2004) 773.
[24] S. Guerin, B.E. Hayden, D. Pletcher, M.E. Rendall, J.-P. Suchsland, J. Comb. Chem. 8 (2006) 679.
[25] A. Sarapuu, M. Nurmik, H. Mändar, A. Rosental, T. Laaksonen, K. Kontturi, D.J. Schiffrin, K. Tammeveski, J. Electroanal. Chem. 612 (2008) 78.
[26] H. Miyamura, R. Matsubara, Y. Miyazaki, S. Kobayashi, Angew. Chem. Int. Ed. 46 (2007) 4151.
[27] C. Lucchesi, T. Inasaki, H. Miyamura, R. Matsubara, S. Kobayashi, Adv. Synth. Catal. 350 (2008) 1996.
[28] G.H. Woehrle, M.G. Warner, J.E. Hutchison, J. Phys. Chem. B 106 (2002) 9979.
[29] M.K. Chow, C.F. Zukoski, J. Colloid Interface Sci. 165 (1994) 97.
[30] K.C. Grabar, K.J. Allison, B.E. Baker, R.M. Bright, K.R. Brown, G. Freeman, A.P. Fox, C.D. Keating, M.D. Musick, M.J. Natan, Langmuir 12 (1996) 2353.
[31] J. Maruyama, M. Inaba, Z. Ogumi, J. Electroanal. Chem. 458 (1998) 175.
[32] N. Alexeyeva, T. Laaksonen, K. Kontturi, F. Mirkhalaf, D.J. Schiffrin, K. Tammeveski, Electrochem. Commun. 8 (2006) 1475.
[33] A. Sarapuu, K. Tammeveski, T.T. Tenno, V. Sammelselg, K. Kontturi, D.J. Schiffrin, Electrochem. Commun. 3 (2001) 446.
[34] E. Higuchi, H. Uchida, M. Watanabe, J. Electroanal. Chem. 583 (2005) 69.
[35] H. Angerstein-Kozlowska, B.E. Conway, A. Hamelin, L. Stoicoviciu, J. Electroanal. Chem. 228 (1987) 429.
[36] H.S. Wroblowa, Y.C. Pan, G. Razumney, J. Electroanal. Chem. 69 (1976) 195.
[37] J.C. Huang, R.K. Sen, E.B. Yeager, J. Electrochem. Soc. 126 (1979) 786.
[38] A. Damjanovic, M.A. Genshaw, J.O'M. Bockris, J. Chem. Phys. 45 (1966) 4057.
[39] M. Huang, Y. Shen, W. Cheng, Y. Shao, X. Sun, B. Liu, S. Dong, Anal. Chim. Acta 535 (2005) 15.